Respiratory Medicine Case Reports 31 (2020) 101239

Contents lists available at ScienceDirect

Respiratory Medicine Case Reports

journal homepage: http://www.elsevier.com/locate/rmcr

Case report

Malignant lymphoma mimics miliary tuberculosis by diffuse micronodular radiographic findings

Kyoko Yagyu *, Masaaki Kobayashi, Takahiro Ueda, Riki Uenishi, Yuko Nakatsuji, Haruhiko Matsushita

Department of Respiratory Medicine, Izumi City General Hospital, Japan

ARTICLE INFO

Keywords:
Diagnostic imaging
Follicular lymphoma
Pulmonary secondary lymphoma
Miliary opacity

ABSTRACT

This case reports rare findings on computed tomography of a manifestation of malignant lymphoma, in which diffuse lung shadows appeared as miliary nodules distributed throughout the lungs bilaterally. The patient had a history of surgical treatment of rectal cancer and had received chemotherapy for suspicious liver metastasis. At her current presentation for evaluation suspected miliary tuberculosis on chest radiography, subsequent liver biopsy revealed a mass infiltration of atypical lymphocytes, which was diagnosed as follicular lymphoma. The miliary tuberculosis was suspected more than neoplastic lesions, such as metastatic rectal cancer or malignant lymphoma. Despite repeated bacteriologic tests of various samples, including sputum, urine, bronchial secretion, peripheral blood, bone marrow aspiration, and gastric lavage, all results were negative for mycobacterium tuberculosis. Finally, multiple, small, mass lesions of lymphocytes were demonstrated in the lung obtained from video-assisted thoracic surgery, and a diagnosis of follicular lymphoma was given. The final interpretations of liver mass and military lung lesions were tumor involvement by the follicular lymphoma. This radiologic findings of multiple miliary opacities throughout the whole lungs confused definite diagnosis because these images were remarkably similar with miliary tuberculous. This case reminds us to consider a wide variety of differential diagnoses even we assumed to be familiar with radiographic imaging at first glance.

1. Background

The pulmonary radiographic finding of malignant lymphoma can appear as various abnormalities, defined as multiple nodules, patchy ground-glass opacities, or consolidation. These individual features are nonspecific; however, they have been reported as manifestations of diseases that commonly involve peribronchovascular distribution with a perilymphatic interstitium [1]. Malignant lymphoma must be included in the differential diagnosis of these abnormal opacities. In this case, the radiographic finding showed bilateral, diffuse, reticulonodular lung lesions, which mimicked miliary tuberculosis. There have been very few reports of such diffuse lung abnormalities in patients with malignant lymphoma in the literature.

2. Case presentation

An 82-year-old woman was referred to the Department of Respiratory Medicine, Izumi City General Hospital, because of a 1-month history of cough and suspected miliary tuberculosis on chest radiography. The patient has a 10-year history of type 2 diabetes. Two years ago, the patient underwent lower anterior resection of the rectum for rectal cancer stage I (pT1bN0M0). One year ago, she was treated for suspected metastatic liver tumors with chemotherapy using 15 cycles of modified FOLFOX6 plus bevacizumab (bevacizumab 5 mg/kg, followed by oxaliplatin 85 mg/m^2, *l*-leucovorin 200 mg/m^2 and bolus infusion of fluorouracil 400 mg/m^2 on day 1 and continuous fluorouracil infusion 2400 mg/m^2 on day 1 through day 2 of a two-week cycle). Because her carcinoembryonic antigen value was normal, ultrasound-guided liver biopsy was performed for histologic confirmation. Ultrasonography showed a partially exophytic hypoechoic lesion in the left medial and right posterior inferior segment of the liver. A diagnostic thick needle biopsy was performed from the lesion in the left medial segment. Pathologic examination showed diffuse proliferation of small lymphocytes with a boundary on the liver tissue (Fig. 1) and positive for CD20 and CD79a. Ultimately, the liver lesions were interpreted as malignant lymphoma.

* Corresponding author. Department of Respiratory Medicine, Izumi City General Hospital, 4-5-1Wake-Cho, Izumi-city, Osaka, 594-0073, Japan.
E-mail address: yagyu604@helen.ocn.ne.jp (K. Yagyu).

https://doi.org/10.1016/j.rmcr.2020.101239
Received 15 June 2020; Received in revised form 17 September 2020; Accepted 19 September 2020
Available online 30 September 2020

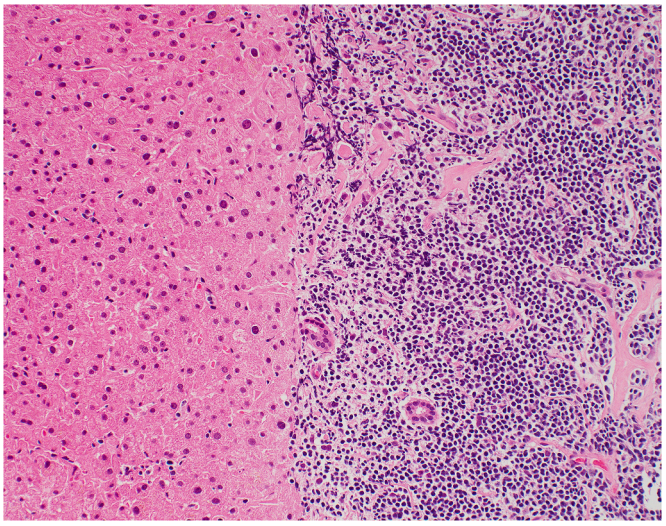

Fig. 1. Histopathological findings of the liver biopsy specimen. The diffuse proliferation of small lymphocytes was observed with a boundary on liver tissue. (hematoxylin and eosin staining, original, × 4).

At her current presentation, miliary deposits throughout the lung bilaterally were demonstrated on chest radiography. Computed tomography of the chest showed innumerable, tiny, well-defined miliary nodules of 1–3 mm diameter in a random distribution pattern, and some of which are distributed in the subpleural (Fig. 2). The "tree-in-bud" appearance was not evident, and no mediastinal lymphadenopathy was detected. Metastatic lung tumor and miliary tuberculosis were in the list of differential diagnoses.

The patient had no cardiac murmur on presentation. Her lungs were clear to auscultation, and abdominal examination was unremarkable with no hepatosplenomegaly. No skin lesions were appreciated; there was no superficial lymphadenopathy.

The patient's C-reactive protein was 0.3 mg/dL, and liver function test results were within the normal range. Tumor markers (carcinoembryonic antigen was 1.0 ng/mL; carbohydrate antigen 19–9 was 3.0 U/mL), Interferon-gamma release assay (T-SPOT.TB, Oxford Immunotec) and angiotensin-converting enzyme levels were within the normal range. The value of lactate dehydrogenase was not elevated at 164 IU/L. The soluble interleukin-2 receptor was slightly elevated at 854 U/mL. Sputum smear for acid-fast bacilli stained negative. Polymerase chain reaction and culture of sputum, urine, and bronchial secretion, in addition to peripheral blood, bone marrow aspiration, and gastric lavage, were all negative for *Mycobacterium tuberculosis*. Furthermore, bronchoalveolar lavage was performed using a total volume of 150 mL of sterile saline solution (56% recovery) from the right posterior bronchus. The bronchoalveolar lavage fluid analysis revealed marked neutrophilia (0.2%), and other cells included lymphocytes (71.2%), eosinophils (0.8%), and macrophages (27.8%), with the total cell count elevated to 1075/μL. The alveolar CD4/CD8 T-cell ratio was high (2.03). Polymerase chain reaction for *Pneumocystis jiroveci* was negative, and the bronchoalveolar lavage fluid yielded no microorganisms.

Transbronchial lung biopsy specimens from the right posterior

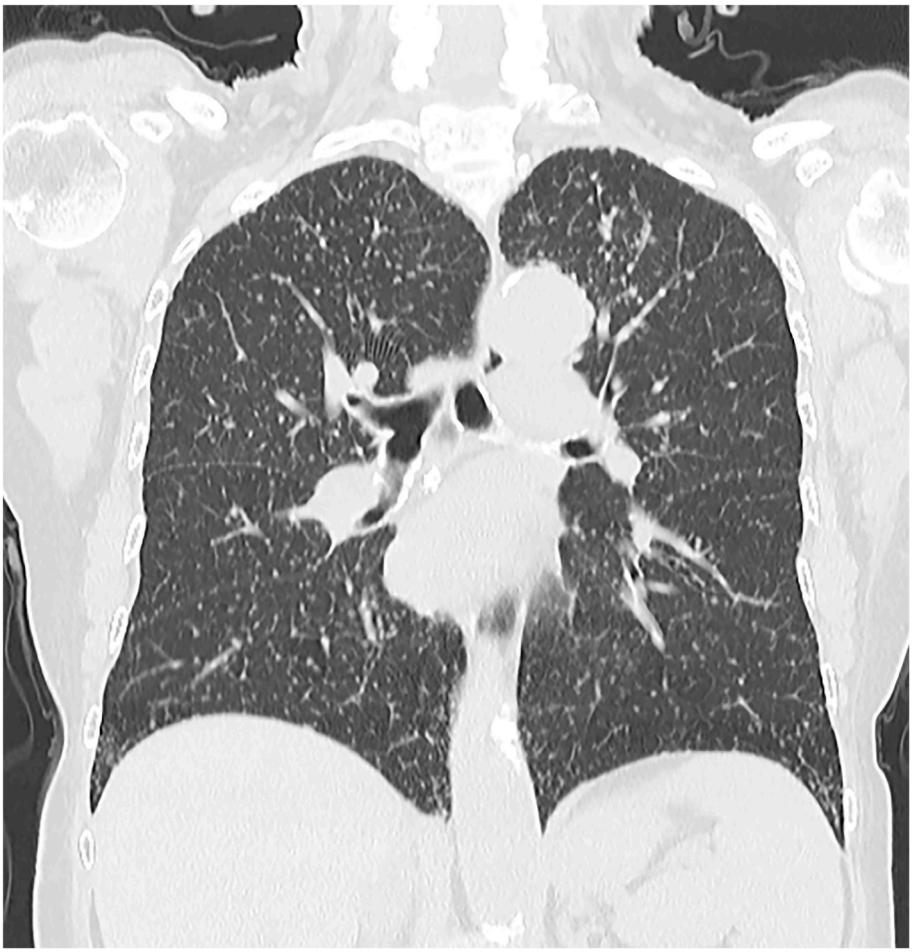

Fig. 2. Computed tomography showing bilateral, diffuse, multiple micronodules in a random distribution pattern, consistent with a miliary pattern throughout both lungs.

segment revealed only lymphocytes with collapsed lung alveolar tissue. Therefore, a thoracoscopic lung biopsy of the middle lobe was performed to rule out metastatic adenocarcinoma from rectum and granulomatous inflammation. Histopathologic examination of biopsied peripheral lung tissue from the posterior segment showed multiple small nodular lesions in pleural area, which composed of lymphoid cells. It scattered the interlobular septum of the lung and pleural (Fig. 3A). In peribronchovascular area (Fig. 3B, hematoxylin-eosin stain and Elastica van Gieson stain), these lymphoid cells found with the bronchovascular bundle, involving submucosa of the bronchiolar trees.

Tumor cells are predominantly composed of monotonous well differentiated lymphocytic type cell, and form follicle structures Grade 1. Immunohistochemical staining of the lymphocytes showed positive results for CD20, CD79a, and CD10. Subsequently, bone marrow studies revealed that lymphoid cells positive for CD20 and CD79a made a cluster of dozens of cells. These pathologic findings completely matched those in the liver biopsy. Whole-body positron emission tomography (PET) revealed increased uptake of 18F-fluorodeoxyglucose (FDG) in the liver lesions located in the left medial segment (26 × 16 mm) and located in right posterior inferior segment (27 × 23 mm), with a maximum standardized uptake value (SUVmax) of 8.7 and 5.1. The SUVmax in lymph node regions of paraaortic left infra-clavicular and mesenteric were >3.3 (Fig. 4). Based on these observations, malignant lymphoma clinical stage IV was diagnosed according to the Cotswolds-modified Ann Arbor classification, involving multiple lung metastases, bone marrow infiltration, metastatic liver tumors, and several lymph nodes. The patient was started on R–CHOP therapy (rituximab 375 mg/m^2, cyclophosphamide 750 mg/m^2, liposomal doxorubicin 50 mg/m^2, vincristine sulfate 1.4 mg/m^2 on day 1 and prednisone 40 mg/m^2 on day 1–5 of a three-week cycle). Complete remission was achieved following 8 cycles of rituximab plus 6 cycles of CHOP therapy, and her symptoms have since been improved. Follow-up is ongoing, and the abnormal radiographic findings have been diminished to date.

3. Discussion

The typical pulmonary imaging is similar in both non-Hodgkin and Hodgkin lymphoma [2]. When metastatic lymphoma involves the lung, the imaging features are varied and nonspecific, such as a solitary nodule; small nodules; peribronchial thickening; multiple, nodular, patchy, ground-glass opacities; and consolidation [1]. These opacities show peribronchovascular distribution with thickening of perilymphatic interstitium [2]. To the best knowledge of these authors, the results of lung imaging for this patient, which mimic miliary tuberculosis, is a rare finding as a manifestation of malignant lymphoma, and thus this case may be educational.

On ultrasound, a malignant lymphoma in the liver is usually well defined and appears markedly hypoechoic because lymphoma is a homogeneous solid tumor and generates very few internal reflections [3].

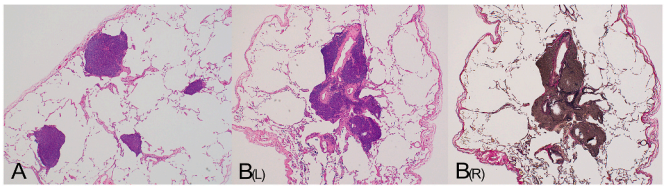

Fig. 3. (A) A biopsy specimen was obtained from the right middle segment and subjected to histopathological analysis. There are multiple small nodular lesions in pleural area, which are composed of lymphoid cells and scattered interlobular septum of the lung and pleural (hematoxylin and eosin staining, × 4). (B) A biopsy specimen was obtained from the right middle segment and subjected to histopathological analysis. In peribronchovascular area, lymphoid cells found along the bronchovascular bundle involving the mucosa along the bronchial and bronchiolar trees extravascularly. (Left: hematoxylin and eosin staining, × 4. Right: hematoxylin-eosin stain and Elastica van Gieson stain, × 4).

According to Okuda's description, for liver tumors <30 mm diameter, it is usually impossible to diagnosis malignant lymphoma based on the ultrasound findings alone. This limitation was because the penetration of vessels within the tumor mass—the characteristic feature of the malignant lymphoma distinguishing from metastatic carcinoma of the liver—is not always demonstrable in tumors <30 mm [4]. The differential diagnosis between malignant lymphoma and metastatic cancer was not possible in the patient in this case study because of the small size of the liver tumors.

In addition, in this case the primary organ of malignant lymphoma could not be determined because of the advanced stage of disease involving multiple lymph nodes (paraaortic, left infraclavicular, and mesenteric), bone marrow, lungs, and liver. It is well known that malignant lymphoma originates from the lymphocytes and involves the liver secondarily. Moreover, the frequency of secondary malignant lymphoma in the liver was about 50% in autopsy cases [5]. Malignant lymphoma, which originates from the lymph node or extra-nodal lymphoid tissue, can involve the liver from the regional lymph nodes. In addition, because the liver produces a large amount of lymph, estimated to be 25%–50% of lymph flowing through the thoracic duct [6], while the main pathway of metastatic liver tumors is via a hematogenous route through either portal or hepatic veins [7]. The CT imaging showed numberless miliary opacity and was similar to miliary tuberculosis, but histopathological analysis revealed that lesions was found in both perilobular and bronchovasular distribution. Lymphoma cells flowing in the peripheral blood and lymphatic system might have spread throughout the whole body from the capillaries, settling in the lymphohematopoietic system, such as lymph nodes, bone marrow, liver. Eventually, they might allow colonizing in the mucosa-associated lymphoid tissue of the bronchi and bronchioles, forming nodules.

4. Conclusion

This case showed follicular lymphoma and intrapulmonary small metastases, which simulated miliary tuberculosis. The radiographic findings of malignant lymphoma are usually nonspecific, and therefore accurate diagnosis of malignant lymphoma of the lung is not usually possible because of such variable radiographic findings. This case is an unusual presentation of follicular lymphoma to the best knowledge of these authors, showing diffuse micronodules on high-resolution computed tomography.

Author's contribution

All persons certify that they have participated sufficiently in the work to take public responsibility for the content, including participation in the concept, design, analysis, writing, or revision of the manuscript. Furthermore, each author certifies that this material or similar material has not been and will not be submitted to or published in any other publication before its appearance in ***Respiratory Medicine Case Reports***.

Kyoko Yagyu: Conceptualization, Methodology, Haruhiko Matsushita: Writing- Original draft preparation, Riki Uenishi and Takahiro Ueda: Resources, Yuko Nakatsuji: Visualization.

Informed consent statement

The patient provided written informed consent.

Funding

The authors received no financial support for the research, authorship, and publication of this article.

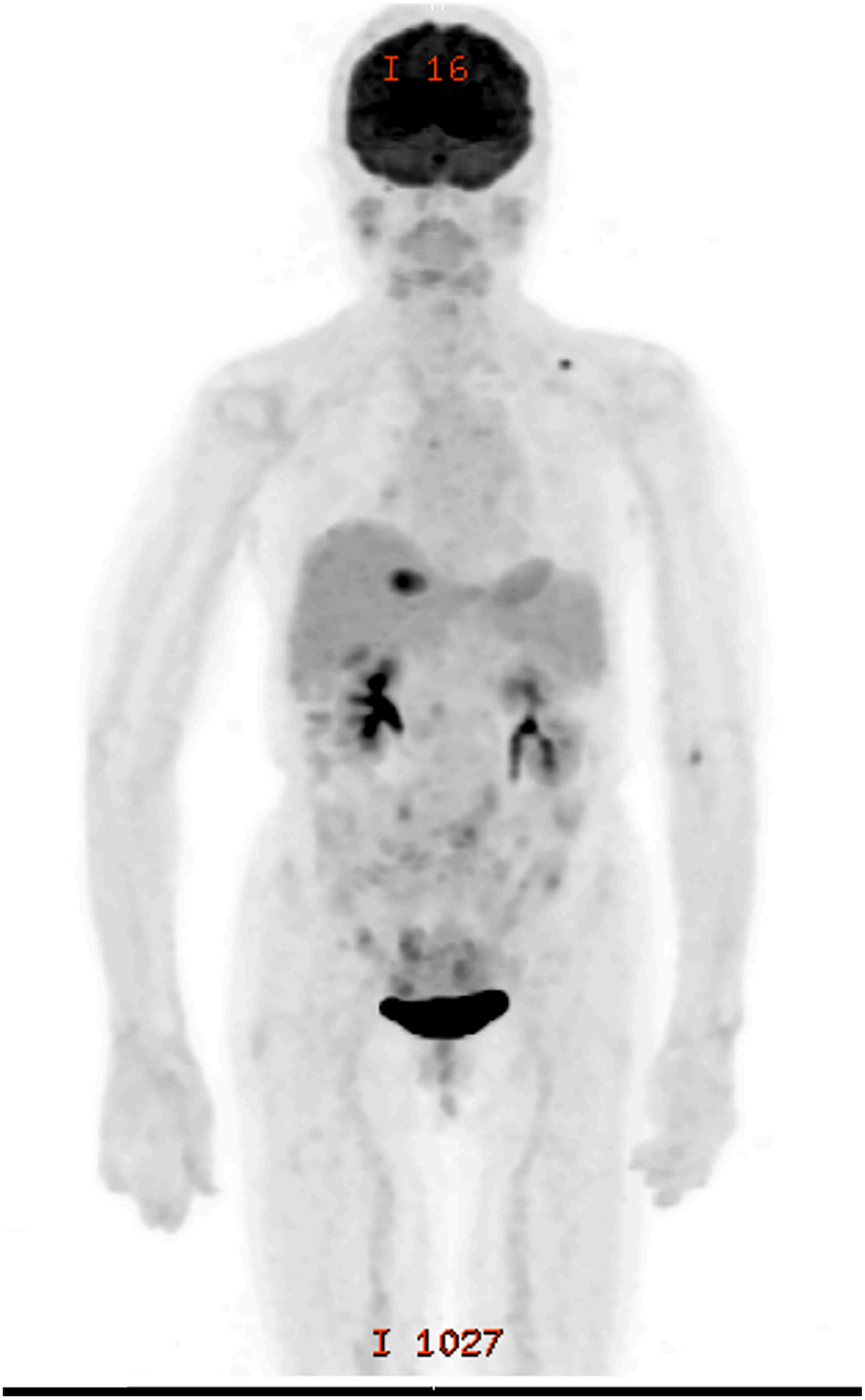

Fig. 4. ^{18}F-FDG PET imaging. 18F-FDG in the liver lesions in the left medial and right posterior inferior segment are SUVmax of 8.7 and 5.1. The SUVmax in lymph node regions of paraaortic left infra-clavicular and mesenteric were >3.3.

Declaration of competing interest

The authors declare that there are no competing interests regarding the publication of this case report.

Acknowledgements

We are grateful to Dr. Kenichi Kakudo, Department of Diagnostic Pathology, Izumi City General Hospital for helpful discussion and pathological diagnosis. I received generous support from Dr. Takayo Ota, Department of Medical Oncology, Izumi City General Hospital, and thank for Enago (www.engo.jp) for carefully proofreading the manuscript.

References

[1] S.S. Hare, C.A. Souza, G. Bain, et al., The radiological spectrum of pulmonary lymphoproliferative disease, Br. J. Radiol. 85 (1015) (2012) 848–864.
[2] C. Freeman, J.W. Berg, S.J. Cutler, Occurrence and prognosis of extranodal lymphomas, Cancer 29 (1) (1972) 252–260.
[3] S. Rajesh, K. Bansal, B. Sureka, et al., The imaging conundrum of hepatic lymphoma revisited, Insights Imaging 6 (6) (2015) 679–692.
[4] Y. Okuda, M. Osugi, Y. Otuka, et al., Ultrasonographic characterization of hepatic malignant lymphoma for effective diagnosis, Jpn. j. Med. Ultrasound Technol. 43 (1) (2018) 22–33 [In Japanese].
[5] M.A. Sistu, U. Baccarani, V. Corno, et al., Primary lymphoma of the liver: a case report and review of the literature, Int. Surg. (83) (1998) 232–234.
[6] O. Ohtani, Y. Ohtani, Lymph circulation in the liver, Anat. Rec. 291 (6) (2008) 643–652.
[7] L. Comparini, Lymph vessels in the liver in man, Angiologica. 6 (5) (1969) 262–274.